Eur Biophys J (1997) 25: 405–410

ARTICLE

R. M. Thomas · A. Zampieri · K. Jumel
S. E. Harding

A trimeric, alpha-helical, coiled coil peptide: association stoichiometry and interaction strength by analytical ultracentrifugation

Received: 29 November 1996 / Accepted: 2 December 1996

Abstract Alpha-helical coiled coils are proving to be almost ideal systems for the modelling of peptide and protein self-association processes. Stable oligomeric systems, in which the stoichiometry is well defined, can be produced by the careful selection of the appropriate amino acid sequence, although the principles behind this are still not fully understood. Here we report on a 35 residue peptide, FZ, synthesized by the solid phase method, which was originally designed to form a dimer, but which, in fact, associates to the trimeric state. A detailed characterization of the associative properties of the peptide has been performed by circular dichroism spectroscopy and, in particular, by sedimentation equilibrium in the analytical ultracentrifuge. The presence of the trimeric state, which is stable even at low peptide concentrations, has been confirmed by various, independent methods of analysis for molar mass. The effects of both temperature and of guanidinium chloride on the peptide have been investigated and both found to be peptide-concentration dependent. The unfolding induced by the denaturant cannot be adequately described by a simple, two state monomer-trimer equilibrium.

Key words α-helical coiled coil · Sedimentation equilibrium · Circular dichroism · Peptide and protein self-association

Abbreviations CD, circular dichroism · GuHCl, guanidinium chloride · HPLC, high performance liquid chromatography · rpm, revolutions per minute

R. M. Thomas (✉) · A. Zampieri
Institut für Polymere, ETH-Zentrum, CH-8092 Zürich, Switzerland
(Fax: +41-1-632-1073; email: rthomas@ifp.mat.ethz.ch)

K. Jumel · S. E. Harding
National Centre for Macromolecular Hydrodynamics,
University of Nottingham, Department of Applied Biochemistry
and Food Science, Sutton Bonington LE12 5RD, UK

Introduction

The utility of the coiled coil motif as a model for the verification of *de novo* protein design principles and for the investigation of protein-protein recognition functions has been well established. Crick suggested that right-handed amphipathic α-helices formed by peptide sequences that consisted of a recurrent hepated of amino acids, containing two hydrophobic residues at well defined positions, could pack efficiently to form left-handed superhelices (Crick 1953). He also noted that there was no strong *a priori* reason to favour a two-stranded rather than a three-stranded structure. Naturally occurring coiled coils include members of both classes (Cohen and Parry 1990) and they also appear in the familiar 4-helical bundle. In fibrous proteins, and in those regions of globular proteins that adopt a similar configuration, the dimeric form appears to predominate. In the latter case the main role of the motif is to provide an oligomerization and recognition interface.

Model coiled coils, in general, have been designed on the basis of information gained from the study of large structural proteins, such as myosin and tropomyosin, or the dimerization region of DNA regulatory proteins, often referred to as a "leucine zipper" (Landschutz et al. 1988), and that of the yeast transcriptional activator GCN4-p1 in particular. They have been used to investigate the helical potential of individual amino acids (O'Neil et al. 1990; Betz et al. 1995), the nature of the internal hydrophobic packing (Zhu et al. 1993, Harbury et al. 1993; DeLano and Brünger, 1994) and the role of electrostatic forces in determining the specificity and strength of interhelical interaction (Hu et al. 1993; Lovejoy et al. 1993; Zhou et al. 1994; Lumb and Kim 1995; Lavigne et al. 1996; Lumb and Kim 1996). Studies of coiled coils in which crystal structures have been obtained (Lovejoy et al. 1993; O'Shea et al. 1991; Harbury et al. 1993) have shown that dimeric, trimetic and tetrameric structures can be found and that the oligomerization state is apparently compositionally determined. It has become clear that one major determinant of dimeric structure in all these model peptides is the pres-

ence of an asparagine residue in a hydrophobic position in the central heptad (Betz et al. 1995; Harbury et al. 1993; Thomas et al. 1995), as is found in GCN4-p1.

The progenitor of many of the model sequences that have been employed is the tropomyosin analogue, TM43, of Hodges and his coworkers (Lau et al. 1984). This sequence was originally believed to form a dimer on the basis of sedimentation equilibrium experiments, but a recent reappraisal, in which an accurate measurement of the partial specific volume of the peptide was made, indicates that it is predominantly a trimer in dilute aqueous solution (Betz et al. 1995).

A peptide with the same sequence as the first 35 residues of TM43 but with one leucine per heptad switched to phenylalanine, FZ ("phenylanaline zipper"), is the subject of this study. It was thought that, on the basis of the then currently available data on TM43, it too would form a dimer, but preliminary hydrodynamic data indicated that it was also trimeric (Thomas et al. 1995). FZ was designed for the investigation of inter-molecular recognition functions and as a candidate for template-directed peptide self-replication and is fully α-helical, as judged by CD spectroscopy. It has the simple, repetitive sequence $(KFEALEG)_5$, synthesized as the N-acetylated C-terminal amide, and has proved to be an ideal model in which to study molecular self-association. This article reports on a detailed investigation into the properties of FZ at sedimentation equilibrium (using both absorption and Rayleigh optical detection systems) in the analytical ultracentrifuge, in which the stable trimeric structure is firmly established and the strength of the interaction is discussed. The hydrodynamic data are reinforced by further CD investigations into the effect of temperature and chemical denaturation on the structure of the peptide.

Materials and methods

Peptide synthesis

FZ was synthesized both manually and automatically by the solid phase method on Rink amide resin, using standard synthesis protocols. The peptide was purified by reversed phase HPLC and the identity of the product was confirmed by electrospray mass spectrometry. The peptide had a monomer molar mass, M_c, of 3933 g · mol^{-1} and a partial specific volume, $\bar{v}_{20,c}$, of 0.746 cm^3 g^{-1} calculated from its amino acid composition (Laue et al. 1992).

Solvent systems

Two solvents of differing pH and ionic strength were employed. (a) 0.01 M sodium phosphate, 0.09 M sodium fluoride, pH 7.0, I = 0.10 M ("phosphate/fluoride" buffer) and (b) 4.595 g $Na_2HPO_4 \cdot 12\ H_2O$, 1.561 g KH_2PO_4, 2.923 g NaCl per litre of deionised, distilled water, pH 6.8, I = 0.10 M (Green 1933). Both buffers were used in the production of guanidinium chloride solutions.

Analytical ultracentrifugation

Sedimentation equilibrium experiments were performed in two types of analytical ultracentrifuge with differing optical systems. (a) The Beckman Optima XL-A ultracentrifuge equipped with scanning absorption optics and full on-line computer data capture and analysis facilities (Beckman, Palo Alto, USA; Giebler 1992). Multi-channel cells of 12 mm optical path length were employed (3 solution/solvent pairs) and the temperatures quoted were those reported by the instrument. Three detection wavelengths were used: 220 nm and 230 nm (amide absorbance) and 257 nm (phenylalanine absorbance). Three independent methods of (weight average) molar mass analysis were employed: MSTARA (Harding et al. 1992), which uses the M^* method (Creeth and Harding 1982) and has recently been computerized (Colfen and Harding 1996), and XLAse, (D. Lechner, personal communication) which is based on the more conventional average determination of d ln c/dr^2, where c is concentration and r the radial distance. Whole cell averages, assuming the presence of a single, ideal species, were also calculated, using software supplied by the instrument manufacturer. (b) A Beckman Model E ultracentrifuge equipped with Rayleigh Interference optics, a laser light source (5 mW, He-NE) and an automatic off-line (i.v. via photographic records) data capture facility (Harding and Rowe, 1989). All measurements were performed at 20 °C and 12 mm optical path length cells were used. Equilibrium concentration distributions were recorded using Rayleigh interference optics with a 632.18 nm, 5 mW He-Ne laser. Optical images were recorded on photographic film and digitalized with a laser densitometer (LKB, Bromma, Sweden). Fringe distributions were converted to a concentration distribution using the routine ANALYSER (Harding and Rowe 1989) and whole distribution weight average, M_w, and point average, M_w (r); molar masses were generated using the routine MSTARI (Harding et al. 1992; Colfen and Harding 1996).

Circular dichroism

CD spectra were measured with a Jasco J-600 spectropolarimeter equipped with a thermostatted cell block.

Results

Analytical ultracentrifugation

The analyses below were based on the assumption that, because of the low protein concentrations used and the small size of the molecular species involved, thermodynamic non-ideality effects were negligible and that the apparent weight average molar mass, $M_{w,\,app}$, approximated the true weight average molar mass, M_w.

Initial measurements were performed in the XL-A ultracentrifuge equipped with uv-absorption optics, in the phos-

phate-fluoride buffer and at low peptide concentration. Nine runs were performed at 3 different cell loading concentrations: 0.0275, 0.138 and 0.275 mg/mL (0.1 mg/mL ≈25 μM), to monitor the effect of concentration on self-association, and at 3 rotor speeds (16,000, 21,000, and 30,000 rpm), the lower speeds being used to check for the presence of any large molecular weight aggregates that might have been missed at higher speed. All methods of M_w analysis gave very similar molar mass values that were independent of rotor speed and peptide concentration and were within the range 11,000±800 g · mol^{-1} (Table 1), consistent with a trimeric molecule. Two further measurements were performed at 50,000 rpm and a scanning wavelength of 230 nm; these too gave similar results: at 0.05 mg/mL M_w=11,400±500 g · mol^{-1} and at 0.2 mg/mL, M_w=12,200±500 g · mol^{-1}.

Having clearly established the stoichiometry of the system and shown that the simple mass action effect of lowering the concentration was unable to shift the associative equilibrium, the influence of the protein denaturant 6M GuHCl was investigated. Unfortunately the solvent was opaque in the far UV so a higher wavelength for detecting the peptide had to be chosen. Higher loading peptide concentrations (0.5 and 1.0 mg/mL) provided a measurable signal at 257 nm, and values for M_w of (4,600±1,000) g/mol and (3,500±1,000) g/mol were obtained for the two respective concentrations at 49,000 rpm and 20.0°C. The material was quite clearly converted to the monomeric form, although the extraction of more quantitative information was not possible because of the limitations of the absorption optics of the XL-A. More detailed analyses (the determination of point average molecular weights, M_w (r), (i.e. M_w, as a function of radial position r) required the use of less convenient but more precise Rayleigh interference optics of the Beckman Model E analytical ultracentrifuge.

To this end, measurements were performed at a loading concentration of 1.5 mg/mL (380 μM) at 30,000 rpm in 0M GuHCl and 48.000 rpm at 2,4 and 6M GuHCl at 20°C. The results as summarised in Table 2 are somewhat surprising. Although 6M GuHCl reduces the mass to that of the monomer, the application of lower concentrations of GuHCl appears to promote further association. Possible variation in partial specific volume in the presence of GuHCl cannot be the explanation since calculations on the data obtained at 6M GuHCl yield the monomeric mass without correction of the $\bar{v}$ value.

This observation was confirmed by plotting point weight average molar mass, M_w (r) as a function of local concentration, expressed in fringe displacement numbers, J (r), for each of the 4 values of [GuHCl] in Table 2 (Fig. 1). These are obtained from local slopes of the conventional log J (r) versus r^2 plots taken at various radial positions (or "points") along the equilibrium concentration distribution. Whereas the 0M and 6M GuHCl profiles in Fig. 1 are as expected, those for the 2M and 4M cases both exhibit a different type of behaviour, the values of log J (r) in 2M GuHCl reaching a plateau at ≈17,500 g · mol^{-1} suggesting the association goes as far as a tetramer or pentamer.

The XL-A instrument was also used to investigate the effect of temperature on $M_{w,\,app}$ over the 20–35°C range in phosphate/fluoride buffer, and the results are shown in Fig. 2. As expected, thermal dissociation is peptide-concentration dependent and, while the effects at low concentration (3 μM) are marked, at high concentration (310 μM)

Table 1 Molecular weight experiments on FZ: sedimentation equilibrium using absorption optics on the XL-A ultracentrifuge. [a] Monomer molar mass, M_w=3933 g · mol^{-1}; [b] from MSTAR analysis; [c] from XLAse analysis

Conc. (mg/mL)	Rotor speed (rpm)	Wavelength (nm)	M_w (g · mol^{-1})[b]	M_w (g · mol^{-1})[c]
0.0275	16000	220	12000±700	12400
0.0275	21000	220	11100±600	11200
0.0275	30000	220	9400±200	9300
0.138	16000	230	11100±500	11500
0.138	21000	230	10700±200	11000
0.138	30000	230	12000±200	12400
0.275	16000	230	11000±100	11500
0.275	21000	230	10200±200	10300
0.275	30000	230	10700±100	10500

Table 2 Effect of increasing [GuHCl] on M_w, investigated using the Model E ultracentrifuge. All measurement made at 20.0°C

[GuHCl] M	M_w (g · mol^{-1})
0	13300±1000
2	15500±3000
4	14200±3000
6	5000±1000

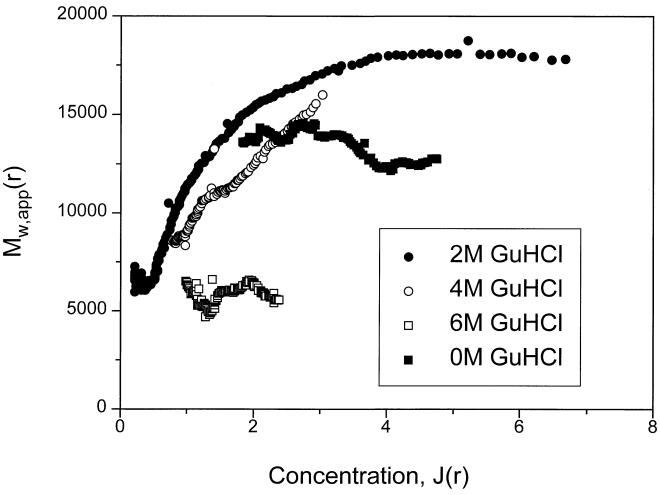

Fig. 1 Effect of increasing [GuHCl] on point weight average molar masses of FZ plotted against fringe displacement, J. A. Beckman Model E ultracentrifuge, equipped with Rayleigh interference optics, was used. Rotor speed 48 000 rpm, loading peptide concentration =1.5 mg/mL (380 μM). All measurements were made at 20.0°C

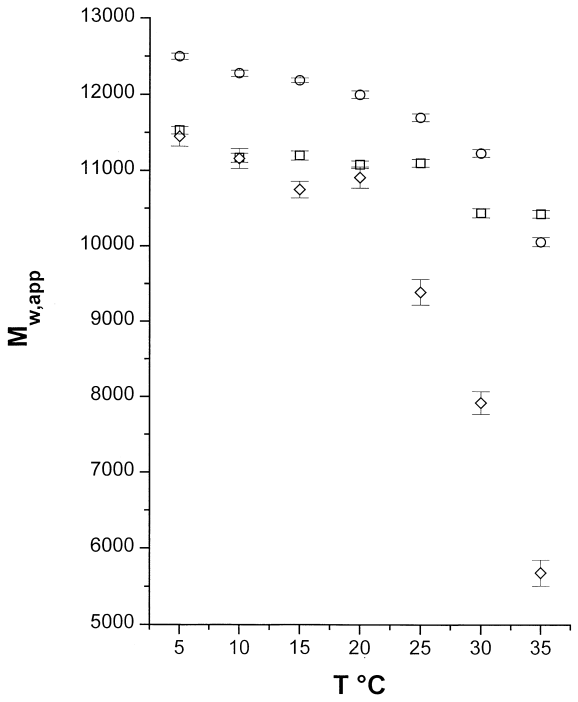

Fig. 2 The dependence of M_w on temperature at peptide concentrations of 310 (□) 31 (○) and 3 μM (◇) in phosphate/fluoride buffer. An XL-A ultracentrifuge was used and the temperatures quoted are those reported by the instrument

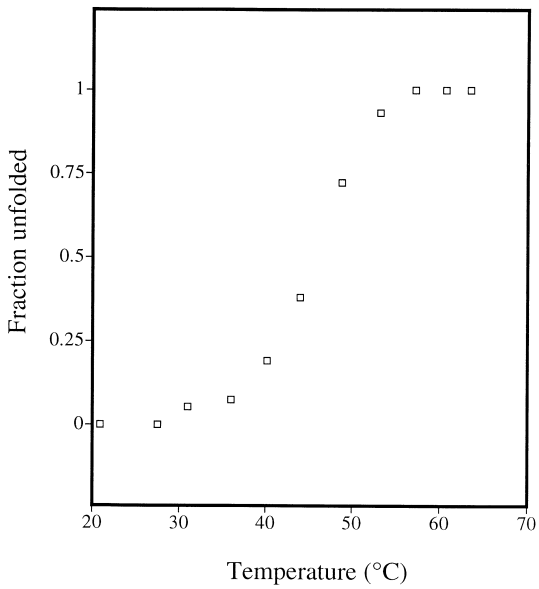

Fig. 3 The thermal denaturation of FZ in phosphate/fluoride buffer; the ellipticity at 222 nm as a function of temperature

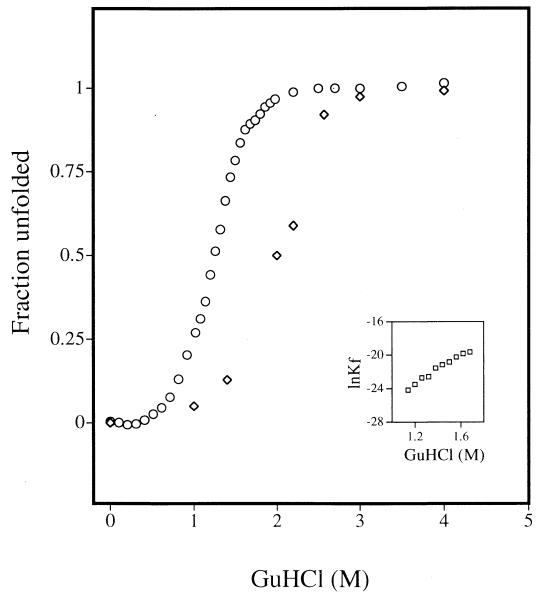

Fig. 4 The GuHCl-induced unfolding of FZ in phosphate/fluoride buffer, 20 °C; ellipticity at 222 nm as a function of [GuHCl] at peptide concentrations of 13 (○) and 270 μM (◇). The inset shows the dependence of $\ln K_f$ on [GuHCl]

only the onset of the dissociation/unfolding transition can be seen. Owing to instrumental limitations on temperature this process could not be followed in more detail.

Circular dichroism

The CD spectrum of FZ is typical of that of a fully helical coiled coil at all accessible peptide concentrations in phosphate/fluoride buffer at 20 °C (Θ_{222} = −30,000 deg · cm^2 · d mol^{-1}). In order to investigate further its stability, and to complement the sedimentation data, the spectrum was measured as a function of temperature in phosphate/fluoride buffer and in differing GuHCl concentrations in the same solvent. The reversibility of both processes was established by either cooling the sample or by diluting the GuHCl containing solutions with buffer, and remeasuring the spectrum. The thermal transition measured at a peptide concentration of 326 μM had a midpoint of ≈ 45 °C and was fully reversible (Fig. 3). This result was compatible with the onset of thermal unfolding seen in the sedimentation data at about the same peptide concentration (Fig. 2). The guanidine-induced denaturation was also peptide-concentration dependent. The complete titration measure at an FZ concentration of 13 μM shown in Fig. 4 was fully reversible, and had a midpoint of ≈ 1.4 M GuHCl. Increasing the peptide concentration to 270 μM has the expected effect of shifting the unfolding midpoint to higher GuHCl concentration, in this case ≈ 2 M.

Discussion

The detailed hydrodynamic results presented here confirm that FZ forms a trimeric coiled coil that is stable even at low peptide concentration. The orientation of the individual monomers is unknown but is suspected to be parallel, by analogy with closely similar systems. The effects of substitution at the hydrophobic positions of coiled coils (sites

a and **d** in the conventional lettering of the heptad) with the larger apolar amino acids are subtle. Double substitution with the same amino acid often leads to the trimeric state, while other associative states, as well as the trimer, are formed when the residues at the **a** and **d** sites differ. Even the normally dimeric GCN4-p1 can be switched to trimeric and tetrameric configurations by mutations in the hydrophobic core (Harbury et al. 1993). Analytical ultracentrifuge and mass spectrometric studies on the related peptide LZ, another analogue of TM43 that, unlike FZ, preserved the same pattern of leucine residues as its parent, showed that it formed a stable trimer (Wendt et al. 1995a, b; Thomas et al. 1995) as did the similar coil-La-Ld peptide (Betz et al. 1995). The results reported here indicate that swapping the first leucine in a heptad for a phenylalanine residue has no effect on the formation of the final oligomeric state.

Dissociative phenomena in self-associating systems are, of course, concentration dependent. While the oligomeric state is often stable even at very low peptide concentration, amino acid substitution can be used to modulate stability. For example, swapping one leucine for an alanine in the central heptad of LZ causes the molecule to dissociate at peptide concentrations below 100 μM, apparently forming a dimer at the limiting concentrations open to sedimentation equilibrium measurement. In contrast, the hydrodynamic data presented here clearly show that there is no significant dissociation of the stable trimeric form of FZ even at the lowest concentrations used, and that therefore, the apparent dissociation constant must be <7 μM. This is consistent with the known stability of coiled coils; the dissociation constant of the homodimeric GCN4-p1 leucine zipper, for example, is ≈ 10 μM or lower (O'Shea et al. 1989). The dissociation of FZ can, however, be induced by raising the temperature or by the introduction of a chemical denaturant. In both cases the process is reversible. Lack of a suitably sensitive optical system and access to only a narrow temperature range has meant that it has not been possible to investigate the full thermal unfolding transition of FZ using the ultracentrifuge, although the results obtained are in agreement with those measured by CD spectroscopy. The GuHCl-induced unfolding of the peptide, as monitored by CD shows no evidence of intermediates, and appears to follow a single, reversible two-state transition. Assuming that this is the case, and that only trimer and monomer are present at equilibrium, an apparent equilibrium constant, K_f, can be estimated as

$$K_f = 3\, C_T^2\, [\, f_u^3/(1 - f_u)]$$

where C_T is the total peptide concentration and f_u the fraction of molecules unfolded. The plot of $\ln K_f$ *vs* [GuHCl], shown in the inset to Fig. 4 is clearly not linear, suggesting that this simple model may not, in fact, be correct, and precluding further estimation of thermodynamic parameters. The point average sedimentation equilibrium data at intermediate GuHCl concentrations are surprising and appear to indicate that the peptide forms higher associated states, that may be either structurally ordered or disordered, before relaxing to the fully unfolded state which would account for the deviation in linearity seen in the CD data. The only plausible explanation of this phenomenon would be that partial unfolding or dissociation of the individual α-helices exposes a further site(s) for self-association, which is subsequently lost as the peptide chains completely denature. This is relatively simple to model if the peptide, or a population thereof, remains fully helical, but is harder to reconcile if the associating species are themselves unfolded. This raises questions as to the precise nature and quantitation of the various species possibly present at equilibrium and as to mechanistic and kinetic aspects of the formation of the oligomeric state.

Two clear mechanisms leading to the formation of a trimer can be postulated. One involves a simple cooperative transition from the monomer while the second implies the presence of a different oligomeric state either transiently or in the population present at equilibrium. It appears that FZ exhibits the latter type of behaviour and a full description of the system will require further kinetic and equilibrium measurements.

Acknowledgements This work was supported by the Engineering and Physical Science Research Council (SEH and KJ) and the Cost D7 Action Chemistry Committee of the EEC (SEH, RT).

References

Betz S, Fairman R, O'Neil K, Lear J, DeGrado W (1995) Design of two-stranded and three-stranded coiled-coil peptides. Phil Trans R Soc Lond B 348:81–88

Cohen C, Parry DAD (1990) α-helical coiled coils and bundles: How to design an α-helical protein. Proteins: Struct Func Genet 7:1–153

Colfen H, Harding SE (1997) MSTAR: An Interactive PC program for the model independent evaluation of sedimentation equilibrium data. Eur Biophys J 96 (this issue)

Crick FHC (1953) The packing of α-helices: simple coiled-coils. Acta Cryst 6:689–697

Creeth JM, Harding SE (1982) Some observations on a new type of point average molecular weight. J Biochem Biophys Meth 7:25–34

DeLano WL, Brünger AT (1994) Helix packing in proteins: prediction and energetic analysis of dimeric, trimeric and tetrameric GCN4 coiled coil structures. Proteins: Struct Funct Genet 20: 105–123

Giebler R (1992) The Optima XL-A: a new analytical ultracentrifuge with a novel precision absorption optical system. In: Harding SE, Rowe AJ, Horton JC (eds) Analytical ultracentrifugation in biochemistry and polymer science. Royal Society of Chemistry, Cambridge, UK, pp 16–25

Green AA (1933) The preparation of acetate and phosphate buffers of known pH and ionic strength. J Am Chem Soc 55:2331–2336

Harbury PB, Zhang T, Kim PS, Alber T (1993) A switch between two-, three-, and four-stranded coiled coils in GCN4 leucine zipper mutants. Science 262:1401–1407

Harding SE, Horton JC, Morgan PJ (1992) MSTAR: A FORTRAN program for the model independent molecular weight analysis of macromolecules using low speed or high speed sedimentation equilibrium. In: Harding SE, Rowe AJ, Horton JC (eds) Analytical ultracentrifugation in biochemistry and polymer science. Royal Society of Chemistry, Cambridge, UK

Hu JC, Newell NE, Tidor B, Sauer RT (1993) Probing the roles of residues at the **e** and **g** positions of the GCN4 leucine zipper by combinatorial mutagenesis. Protein Sci 2:1072–1084

Landschulz WH, Johnson PF, McKnight SL (1988) The leucine zipper: A hypothetical structure common to a new class of DNA binding proteins. Science 240:1759–1764

Lau SYM, Taneja AK, Hodges RS (1984) Synthesis of a model protein of defined secondary and quaternary structure. J Biol Chem 259:13253–13261

Laue TM, Shah BD, Ridgeway TM, Pelletier SL (1992) Computer-aided interpretation of analytical sedimentation data for proteins. In: Analytical sedimentation data for proteins. In: Analytical ultracentrifugation in biochemistry and polymer science. Royal Society of Chemistry, Cambridge, UK, pp 90–125

Lavigne P, Sönnichsen FD, Kay CM, Hodges RS (1996) Interhelical salt bridges, coiled coil stability and specificity of dimerization. Science 271:1136–1137

Lumb KJ, Kim PS (1995) Measurement of interhelical electrostatic interactions in the GCN4 leucine zipper. Science 268:436–439

Lumb KJ, Kim PS (1996) Interhelical salt bridges, coiled coil stability and specificity of dimerization. Science 271:1137–1138

Lovejoy B, Choe S, Cascio D, McRorie DK, DeGrado WF, Eisenberg D (1993) Crystal structure of a synthetic triple-stranded α-helical bundle. Science 259:1288–1293

O'Neil KT, DeGrado WF (1990) A thermodynamic scale for the helix-forming tendencies of the commonly occurring amino acids. Science 250:646–651

O'Shea EK, Rutkowski R, Kim PS (1989) Evidence that the leucine zipper is a coiled coil. Science 243:538–541

O'Shea EK, Klemm JD, Kim PS, Alber T (1991) X-ray structure of the GCN4 leucine zipper, a two-stranded, parallel coiled coil. Science 254:539–544

Thomas RM, Wendt H, Zampieri A, Bosshard HR (1995) α-helical coiled coils: simple models for self-associating peptide and protein systems. Prog Colloid Polymer Sci 99:24–30

Wendt H, Berger C, Baici A, Thomas RM, Bosshard HR (1995a) Kinetics of folding of leucine zipper domains. Biochemistry 34:4097–4107

Wendt H, Dürr E, Thomas RM, Przybylski M, Bosshardt HR (1995b) Characterization of leucine zipper complexes by electrospray ionization mass spectrometry. Protein Sci 4:1563–1570

Zhou NE, Kay CM, Hodges RS (1994) The role of interhelical ionic interactions in controlling protein folding and stability. J Mol Biol 237:500–512

Zhu B-Y, Zhou NE, Kay CM, Hodges RS (1993) Packing and hydrophobicity effects on protein folding and stability: Effects of β-branched amino acids, valine and isoleucine, on the formation and stability of two-stranded α-helical coiled coils/leucine zippers. Prot Sci 2:383–394